The d3Π state of LiRb

I. C. Stevenson, D. B. Blasing, A. Altaf, Y. P. Chen, and D. S. Elliott

Citation: The Journal of Chemical Physics **145**, 224301 (2016); doi: 10.1063/1.4964655
View online: http://dx.doi.org/10.1063/1.4964655
View Table of Contents: http://scitation.aip.org/content/aip/journal/jcp/145/22?ver=pdfcov
Published by the AIP Publishing

The $d\ ^3\Pi$ state of LiRb

I. C. Stevenson,[1,a)] D. B. Blasing,[2,a)] A. Altaf,[3] Y. P. Chen,[1,2,4] and D. S. Elliott[1,2,4]
[1]*School of Electrical and Computer Engineering, Purdue University, West Lafayette, Indiana 47907, USA*
[2]*Department of Physics and Astronomy, Purdue University, West Lafayette, Indiana 47907, USA*
[3]*Intel Corp., Portland, Oregon 97124, USA*
[4]*Purdue Quantum Center, Purdue University, West Lafayette, Indiana 47907, USA*

(Received 15 July 2016; accepted 28 September 2016; published online 8 December 2016)

We report our spectroscopic studies of the $d\ ^3\Pi$ state of ultra-cold $^7Li^{85}Rb$ using resonantly enhanced multi-photon ionization and depletion spectroscopy with bound-to-bound transitions originating from the metastable $a\ ^3\Sigma^+$ state. We evaluate the potential of this state for use as the intermediate state in a stimulated-Raman-adiabatic-passage transfer scheme from triplet Feshbach LiRb molecules to the $X\ ^1\Sigma^+$ ground state and find that the lowest several vibrational levels possess the requisite overlap with initial and final states, as well as convenient energies. Using depletion measurements, we measured the well depth and spin-orbit splitting. We suggest possible pathways for short-range photoassociation using deeply bound vibrational levels of this electronic state. *Published by AIP Publishing.* [http://dx.doi.org/10.1063/1.4964655]

I. INTRODUCTION

Ultra-cold molecules can play important roles in studies of many-body quantum physics,[1] quantum logic operations,[2] and ultra-cold chemistry.[3] In our recent studies of LiRb, motivated largely by its large permanent dipole moment,[4] we have explored the generation of these molecules in a dual species magneto-optical trap (MOT).[5,6] In particular, we have found that the rate of generation of stable singlet ground state molecules and first excited triplet state molecules through photoassociation, followed by spontaneous emission decay, can be very large.[7–9] There have been very few experimental studies of triplet states in LiRb,[8] in part because they are difficult to access in thermally distributed systems. Triplet states of bi-alkali molecules are important to study for two reasons: first, Feshbach molecules, which are triplet in nature, provide an important association gateway for the formation of stable molecules;[10] also, photoassociation (PA) of trapped colliding atoms is often strongest for triplet scattering states. Mixed singlet-triplet states are usually required to transfer these molecules to deeply bound singlet states.

We show an abbreviated set of potential energy curves (PEC), as calculated in Ref. 11, in Fig. 1. The d $^3\Pi$ − D $^1\Pi$ (or alternatively the (2) $^3\Pi$ − (2) $^1\Pi$) complex in LiRb, asymptotic to the Li 2p $^2P_{3/2,1/2}$ + Rb 5s $^2S_{1/2}$ free atom state, has several features that can promote its utility in stimulated-Raman-adiabatic-passage (STIRAP) and photoassociation. First, the *ab initio* calculations of Ref. 11 predict mixing between low vibrational levels of the $d\ ^3\Pi_1$ and the D $^1\Pi$ states. Second, both legs of a STIRAP transfer process from loosely bound triplet-character Feshbach molecules to the rovibronic ground state can be driven with commercially available diode lasers. And third, similar deeply bound $^3\Pi$ resonances have been successfully used for short-range PA in RbCs.[12–14] While an interesting discovery on its own, spontaneous decay of these states after PA can populate the $a\ ^3\Sigma^+\ v'' = 0$ state; one RbCs team[13] found spontaneous decay of these states even populated the $X\ ^1\Sigma^+\ v'' = 0$ state.

In the present work, we study the $d\ ^3\Pi_\Omega$ states of LiRb, from the asymptote to the most bound vibrational level. We have found signatures of state mixing between low-lying vibrational levels of the d $^3\Pi_1$ and D $^1\Pi$ levels. We have determined the term energies of the different spin-orbit components of the $d\ ^3\Pi$ state, as well as their vibrational energies. We have also observed alternation of the intensities of the rotational lines, and determined the rotational constants of the lowest vibrational levels.

II. EXPERIMENT

We have previously described the details of our experimental apparatus[15] and provide here only a brief summary. We trap ~5×10^7 Li atoms and ~2×10^8 Rb atoms in a dual species magneto-optical trap (MOT), $\lesssim$1 mK in temperature and 1 mm in diameter.[8] Our Rb MOT is a spatial dark SPOT MOT.[16] We photoassociate Li and Rb atoms to form LiRb molecules using either a 300 mW cw Ti:sapphire laser or a 150 mW cw external cavity diode laser. After spontaneous decay to a distribution of vibrational levels of the $a\ ^3\Sigma^+$ state, we use two-color resonantly enhanced-multi-photon-ionization (RE2PI) to ionize the molecules. The lasers that we use to drive the RE2PI process are a Nd:YAG-pumped, pulsed dye laser (PDL) for the first photon, tunable in the wavelength range between 667 nm and 750 nm (14 950-13 300 cm^{-1} frequency range) and part of the 532 nm pump laser for the second photon. The repetition rate of this system is 10 Hz, and it delivers ~1.5 mJ/pulse of dye energy in a 4 mm diameter beam and a larger ~2 mJ/pulse 532 nm beam to the MOT region. When the frequency of the

[a)]I. C. Stevenson and D. B. Blasing contributed equally to this work.

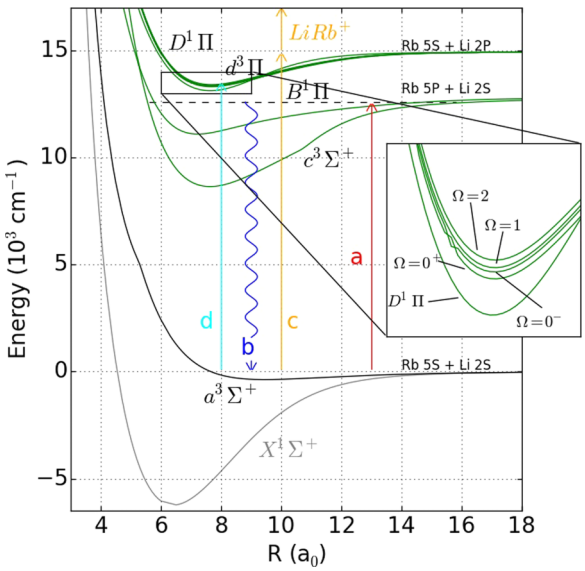

FIG. 1. Energy level diagram of the LiRb molecule, showing relevant PECs from Ref. 11. Vertical lines show the various optical transitions, including (a) photoassociation of atoms to molecular states below the D_1 asymptote; (b) spontaneous decay of excited state molecules leading to the $a\ ^3\Sigma^+$ state; (c) RE2PI to ionize LiRb molecules (ν_c used later in this paper is the frequency of this laser source); and (d) state-selective excitation of the $a\ ^3\Sigma^+$ state for depletion of the RE2PI signal (with laser frequency ν_d). The black dashed line represents our PA states. The inset shows an expanded view of the different $d\ ^3\Pi$ spin-orbit split states as well as the perturbing neighbor $D\ ^1\Pi$.

dye laser is resonant with a transition from an initial state (populated through spontaneous decay from the PA state) to an intermediate bound state (in this experiment the $d\ ^3\Pi$ state), absorption of a dye photon and a 532 nm photon ionizes the molecule. We detect the molecular $LiRb^+$ ions using a time-of-flight spectrometer and a microchannel plate detector. In this paper, we will adopt the following notation: v'' and J'' denote the vibrational and rotational levels of the $a\ ^3\Sigma^+$ and $X\ ^1\Sigma^+$ states, v and J (without a prime) denote the vibrational and rotational levels of the PA resonances (and for these vibrational numbers, we count down from the asymptote using negative integers), and v' and J' denote vibrational and rotational labeling of other excited electronic states.

We used two techniques, RE2PI and depletion spectroscopy, to measure the $d\ ^3\Pi$ bound states. In RE2PI spectroscopy, we tune the PA laser to either the $v = -11$ or $v = -8$ lines of the $2(0^-)$ long range state, from which spontaneous decay leads primarily to the vibrational levels of the $a\ ^3\Sigma^+$ state.[8] We count the number of ions detected over the course of 100 laser pulses and tune the laser frequency ν_c of the PDL in 0.35 cm^{-1} increments. We record the number of ions detected, normalized by the number of laser pulses, as a function of the PDL frequency ν_c.

In order to reach the full range of vibrational levels of the $d\ ^3\Pi$ states, we used two different laser dyes in the PDL. An LDS 698 dye covered the 13 950-14 950 cm^{-1} range, and an LDS 750 dye covered from 13 300 to 13 950 cm^{-1}. These dyes are difficult to work with because of short lifetimes and low power output. The LDS 750 dye in particular was very troublesome: it has a lifetime ≤8 h and produces low power (≤0.5 mJ/pulse for much of its range) and because it has a very broad pulse width (i.e., lots of spontaneous emission), the baseline noise of our RE2PI spectra is enhanced over what we have observed with other dyes.

The $2(0^-)$ $v = -11$ PA line at $\nu_a = 12\,516.89$ cm^{-1} is relatively weak, but it decays almost exclusively to a single vibrational level ($v'' = 11$) of the $a\ ^3\Sigma^+$ state. This facilitates straightforward identification of the vibrational levels of the intermediate state. Unfortunately, several vibrational levels of the $d\ ^3\Pi$ state do not appear in this spectrum, presumably due to poor Franck-Condon overlap with the $v'' = 11$ state. This problem was even more evident when using the LDS 750 dye in the PDL. For this reason, we collected several RE2PI spectra using the stronger $2(0^-)$ $v = -8$ PA resonance $\nu_a = 12\,557.60$ cm^{-1}. This line decays to a wider spread of $a\ ^3\Sigma^+$ vibrational levels, giving more complete coverage of the vibrational lines of the $d\ ^3\Pi$ states, but also making our analysis more difficult, due to the increased congestion of the spectra and frequent overlap between individual lines.

To explore the deeply bound levels of the $d\ ^3\Pi$ states, we used a depletion spectroscopy technique. In these measurements, we used the 150 mW ECDL tuned to the $2(0^-)$ $v = -5$ PA resonance at $\nu_a = 12\,575.05$ cm^{-1}.[8] Spontaneous decay of this state populates the $a\ ^3\Sigma^+$ $v'' = 13$ state. We tune the PDL laser frequency to the (3) $^3\Pi_0$ $v' = 6 \leftarrow a\ ^3\Sigma^+$ $v'' = 13$ one-color resonantly enhanced two-photon ionization (REMPI) transition at 17 736.6 cm^{-1}.[8] We then tune the frequency of the Ti:sapphire laser into resonance with bound-to-bound transitions from the $a\ ^3\Sigma^+$ $v'' = 13$ state to ro-vibrational levels in the $d\ ^3\Pi$ state. Exciting these transitions depletes the population of the $a\ ^3\Sigma^+$ $v'' = 13$ state, causing the REMPI signal to decrease.

III. RE2PI MEASUREMENTS

We show an example of a RE2PI spectrum in Fig. 2. Transitions observed in this spectrum are $d\ ^3\Pi_\Omega$ $v' \leftarrow a\ ^3\Sigma^+$ $v'' = 11$. We have marked the transitions to the $\Omega = 2$ progression with black solid lines, $\Omega = 1$ with blue dashed lines, and $\Omega = 0$ with green dotted-dashed lines. Ω is the total electronic angular momentum, orbital L + spin S, projected onto the internuclear axis. The numerical label for each peak is the vibrational number v' of the $d\ ^3\Pi_\Omega$ state. We have also marked three lines in this spectrum corresponding to transitions to the $D\ ^1\Pi$ state with red dotted lines.

From the spectrum of these $d\ ^3\Pi$ states, we observe the typical hierarchy of line spacings: the vibrational splitting is large (on the order of 100 cm^{-1} for low vibrational quantum number v', and decreasing with increasing v') and the spin-orbit splitting between different Ω states is smaller (on the order of 30 cm^{-1}). The rotational splitting for low J' (on the order of 0.1 cm^{-1}) is too small to be resolved in these RE2PI spectra since the spectral resolution of the PDL is ~0.5 cm^{-1}.

The appearance of transitions belonging to vibrational levels of the $D\ ^1\Pi$ electronic state in Fig. 2 is evidence of mixing between the $D\ ^1\Pi$ and the $d\ ^3\Pi_1$ potentials near an

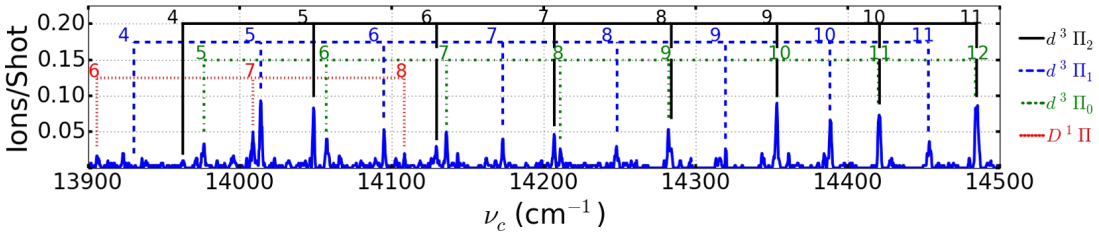

FIG. 2. Subsection of the RE2PI spectra. The PA laser is tuned to the $2(0^-)$ $v = -11$ resonance, from which spontaneous decay is primarily to the $a\ ^3\Sigma^+$ $v'' = 11$ state. Most of these lines are $d\ ^3\Pi_\Omega$ $v' \leftarrow a\ ^3\Sigma^+$ $v'' = 11$ transitions, where v' is labeled on individual lines. From top to bottom: black solid lines label transitions to $\Omega = 2$, blue dashed lines label transitions to $\Omega = 1$, and green dotted-dashed lines label transitions to $\Omega = 0$. Also shown (red dotted lines) are three $D\ ^1\Pi$ $v' \leftarrow a\ ^3\Sigma^+$ $v'' = 11$ transitions.

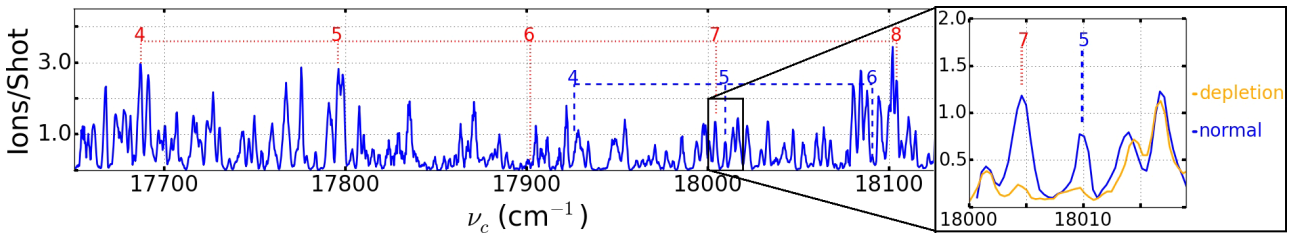

FIG. 3. Subsection of REMPI data with the PA laser tuned to the 4(1) $v = -16$ $J = 1$ resonance,[7] while scanning the REMPI laser frequency, ν_c. Transitions are labeled as $d\ ^3\Pi_1$ $v' \leftarrow X\ ^1\Sigma^+$ $v'' = 10$ (blue dashed) and $D\ ^1\Pi$ $v' \leftarrow X\ ^1\Sigma^+$ $v'' = 10$ (red dotted). The inset shows confirmation of the assignments with depletion spectroscopy. The orange curve in the inset is the REMPI data retaken in the presence of a depletion laser tuned to the $A\ ^1\Sigma^+$ $v' = 25$ $J' = 1 \leftarrow X\ ^1\Sigma^+$ $v'' = 10$ $J'' = 0$[17] transition; the reduction in peak height confirms the assignments. Because the depletion laser reduces the population available for REMPI in both peaks, they must have the same initial state, from which we conclude that we can access triplet REMPI resonances from singlet states.

avoided crossing between the two states. The energy of these $D\ ^1\Pi$ states is known from Refs. 18 and 19. State mixing gives these states partial character of each electronic state, which in this case manifests itself through strong transitions from a triplet state (i.e., $a\ ^3\Sigma^+$ $v'' = 11$) to singlet states ($D\ ^1\Pi$ $v' = 6$–8). This state mixing also adds $D^1\Pi$ character to the $d\ ^3\Pi_1$ states, so one should expect the nearby $d\ ^3\Pi_1$ states to appear in the singlet spectra. This expectation is borne out in the spectrum shown in Fig. 3. This spectrum is a REMPI scan generated in our system after photoassociating ultracold LiRb molecules through a 2(1)–4(1) mixed state at $\nu_a = 12\,574.85$ cm^{-1},[7] which spontaneously decays to vibrational levels of the $X\ ^1\Sigma^+$ ground electronic state. The spectrum in Fig. 3 primarily shows transitions to low-lying $D\ ^1\Pi$ vibrational levels from $X\ ^1\Sigma^+$ $v'' = 10$. We also observe in this spectrum $d\ ^3\Pi_1$ $v' = 4$, 5, and 6 $\leftarrow X\ ^1\Sigma^+$ $v'' = 10$ transitions. We chose $X\ ^1\Sigma^+$ $v'' = 10$ because it is strongly populated by spontaneous decay of the 2(1) - 4(1) PA resonance and transitions to deeply bound $D\ ^1\Pi$ vibrational levels are clearly identified. We can estimate the degree of mixing based on the relative strength of the different REMPI peaks. The $D\ ^1\Pi$ $v' = 7 \leftarrow X\ ^1\Sigma^+$ $v'' = 10$ transition is twice as strong as the $d\ ^3\Pi_1$ $v' = 5 \leftarrow X\ ^1\Sigma^+$ $v'' = 10$ transition so there is twice as much singlet character to $D\ ^1\Pi$ $v' = 7$ as $d\ ^3\Pi_1$ $v' = 5$. Following the same procedure that we have used in the past,[7] we can estimate the interaction strength to be about 7 cm^{-1}. Interestingly, this rough estimate is consistent with the following simple perturbative argument. The spin-orbit interaction responsible for the state mixing can be estimated as about one half the spin orbit mixing in atomic rubidium,[20] or about 120 cm^{-1}. The Franck-Condon factor (FCF) between $D\ ^1\Pi$ $v' = 7$ and $d\ ^3\Pi_1$ $v' = 5$, as calculated by LEVEL 8.0[21] using the PEC from Ref. 11, is about 0.08 and thus the strength of interaction between these states should be approximately 10 cm^{-1}. We have applied this perturbative analysis to each of the vibrational levels of the $d\ ^3\Pi_1$ state (not including $v' = 5$) and find that each contains some small component of $D\ ^1\Pi$ perturber state, on the order of 10% or smaller. This is too small to be seen in the spectra of Fig. 2, but could be sufficient to be useful in a Raman or STIRAP transfer of population to low lying levels of the electronic ground state in the future.

Many of the RE2PI spectra that we collected are less clear than that shown in Fig. 2. In particular, the peaks in the RE2PI spectra near the Rb 5S + Li 2P asymptote are strong, but line congestion becomes significant, and clear identification of the lines in this region becomes difficult. These assignments could probably be improved using a spectroscopic technique that is capable of higher spectral resolution, such as photoassociative spectroscopy, but this was beyond the scope of the present work. Assigning peaks in the RE2PI spectra was equally difficult for deeply bound vibrational states (i.e., $v' \leq 4$). In fact we were unable to observe a clear cutoff in our RE2PI data corresponding to $v' = 0$. We attribute this to difficulties with the LDS 750 dye, specifically the large spontaneous emission content in the pulse. To rectify this problem, we turned to a second set of measurements, based upon depletion spectroscopy.

IV. DEPLETION MEASUREMENTS

We used depletion spectroscopy to identify the lowest two vibrational levels of the $d\ ^3\Pi$ state. Compared to RE2PI,

depletion spectra are sparse and have narrow peak widths, in this case ~1 GHz, a typical linewidth for this type of measurement at this intensity.[22] Additionally, rotational constants can be extracted from depletion spectra,[23] a very useful tool for comparing experiment to theory.

We show depletion spectra for $v' = 0$ in Fig. 4. To assign these data care must be taken with selection rules for radiative transitions in molecules. The two that apply here are $\Delta J = 0, \pm 1$ and $- \leftrightarrow +$, that is, positive symmetry states (with respect to coordinate inversion) must transition to negative symmetry states and vice versa. The initial state in this depletion transition is a $^3\Sigma^+$ state, which is a strict Hund's case (b) state. As such, its rotational energy is determined by quantum number K, which designates the total angular momentum of the molecule apart from spin, rather than the total angular momentum (including spin) quantum number J. For this $a\ ^3\Sigma^+$ state, the electronic spin is $S = 1$, and levels with $J = K + 1, K$, and $K - 1$ are nearly degenerate for $K \geq 1$. Additionally K determines the symmetry of the state.

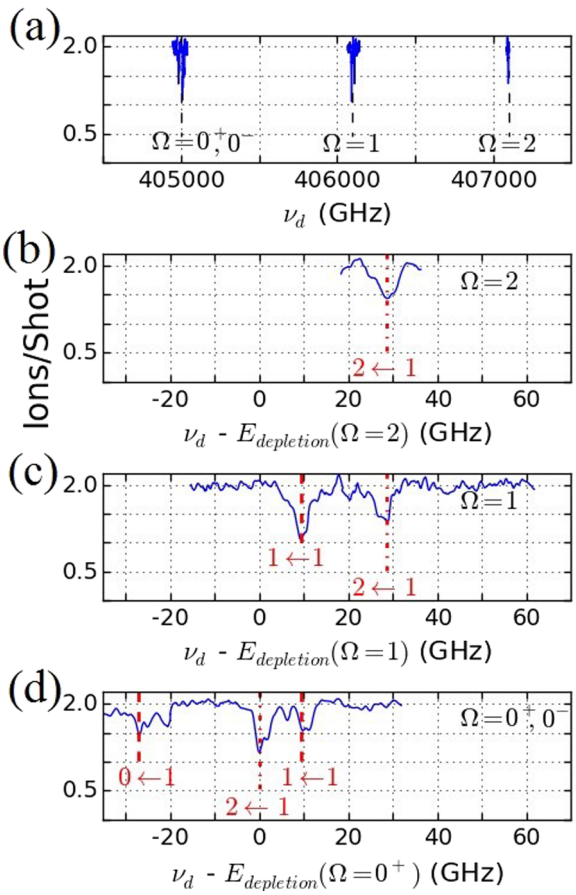

FIG. 4. Depletion spectra of an $a\ ^3\Sigma^+\ v''=13$ REMPI line using the $d\ ^3\Pi\ v'=0$ state. The PA laser is locked to the $2(0^-)\ v=-5$ line, the REMPI laser is tuned to the (3) $^3\Pi_0\ v'=6 \leftarrow v''=13$ transition at $\nu_c = 17\,736.6\ \text{cm}^{-1}$. Panel (a) shows a global view of our depletion data. Panels (b)–(d) show the rotational structure of the depletion lines. All repeatable transitions are labeled $J' \leftarrow J''$. For this $J''=1$ ground state, we assign it to the $K''=0$, even parity manifold. The abscissa of (b)–(d) is the depletion laser frequency offset by $E_{depletion} = T_{0,\Omega} - T_{13}$, where $T_{0,\Omega}$ is the rotationless energy of the $d\ ^3\Pi_\Omega\ v'=0$ state, and T_{13} is the binding energy of the $a\ ^3\Sigma^+\ v''=13$ state, assuming $K''=0$ is the correct assignment.

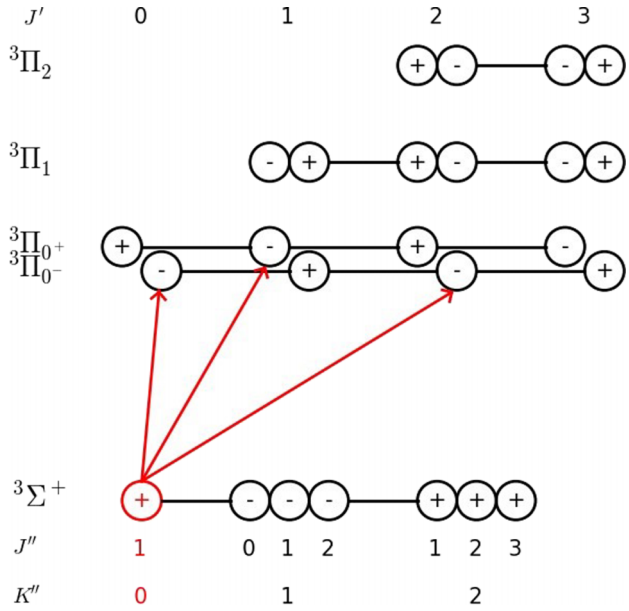

FIG. 5. Rotational structure and parity of $^3\Sigma^+$ and $^3\Pi$ vibrational states, the state in red highlights the ground state we populate at the beginning of the depletion process. Transitions from the populated ground states to $^3\Pi_{0^+}$ and $^3\Pi_{0^-}$ are shown by arrows. Transitions to the negative symmetry levels of $^3\Pi_1$ and $^3\Pi_2$ do occur, but are omitted for clarity. The rotational splitting in $^3\Sigma^+$ is determined by $E = B_v K''(K''+1)$ (which makes the J manifold within each K'' state degenerate) and in $^3\Pi$ by $E = B_v[J(J+1) - \Omega^2]$. Adapted and modified from Ref. 24.

This is summarized in Fig. 5, adapted and modified from Ref. 24.

The logic that leads to our assignments in Fig. 4 goes as follows. We start with the depletion data on transitions to $\Omega = 1$ shown in Fig. 4(c), which is extensive enough to show that (1) the spectrum contains only these two peaks; (2) these two peaks are the $J' = 1$ and 2 rotational states of $\Omega = 1$ (we return to this identification later in this paragraph); and (3) there is no peak corresponding to a transition to $J' = 3$. Since we do see transitions to $J' = 1$ and 2, we know that we populate some mix of $J'' = 0$ and 1 belonging to either $K'' = 0$, 1, or 2. The presence of only two peaks suggests that only *one* of these K'' levels is populated. We assign K'' to be 0, based on (1) the expected dominance of the s-wave scattering state,[25] (2) the clear population in even-symmetry ground states through two-photon couplings from the scattering state in other unrelated measurements in our laboratory,[7,26] and (3) the absence of any peaks for $J' > 2$. The spacing between the two peaks in this spectrum should be $4B_0$, where B_0 is the rotational constant of the $d\ ^3\Pi\ v' = 0$ state, allowing us to determine $B_0 = 4.59$ GHz. This rotational constant agrees with the prediction from LEVEL 8.0 with PECs from Ref. 11, which confirms our assignments of the $d\ ^3\Pi$ state and guides our interpretation of the $\Omega = 0$ data shown in Fig. 4(d), in which we see three transitions. The first two are spaced by $6B_0$ (27.5 GHz), implying that these peaks are transitions to the negative symmetry levels of the $\Omega = 0^-$ electronic state, $J' = 0 \leftarrow J'' = 1$ and $J' = 2 \leftarrow J'' = 1$. The absence of a peak for $J' = 1$ is consistent with the selection rule $+ \leftrightarrow +$. The remaining transition in $\Omega = 0$ must be the only allowed transition to $\Omega = 0^+$, that is, $J' = 2 \leftarrow J'' = 1$. There

TABLE I. Experimental assignments for T_v, the rotationless energy, and B_v, the rotational constant, of the vibrational levels of the $d\ ^3\Pi$ state based on our depletion data for $v' = 0$ and 1. Uncertainty for all T_v is 0.5 cm^{-1}, and uncertainty in the last digit in B_v is given in parentheses. Blank entries denote rotational constants or energies that we were not able to measure because of either the tuning range of our Ti:sapphire laser or because of bound to bound selection rules limited by our PA state.

	$d\ ^3\Pi_{0^-}$		$d\ ^3\Pi_{0^+}$		$d\ ^3\Pi_1$		$d\ ^3\Pi_2$	
v'	T_v (cm^{-1})	B_v (cm^{-1})	T_v (cm^{-1})	B_v (cm^{-1})	T_v (cm^{-1})	B_v (cm^{-1})	T_v (cm^{-1})	B_v (cm^{-1})
0	13 507.9	0.148 (4)	13 508.8		13 544.7	0.153 (6)	13 577.6	
1	13 606.8	0.146 (4)	13 607.6					

is only one transition in $\Omega = 2$, which is trivial to identify as $J' = 2 \leftarrow J'' = 1$.

This assignment suggests that the previous assignment of rotational quantum number of the different vibrational levels of the $2(0^-)$ through which we photoassociate the molecules is incorrect. In Refs. 5 and 8, we had tentatively identified these states as $J = 1$, which is an even parity state. In that work, however, we could observe only one rotational state, so that rotational assignment was weak. It now appears that odd parity $J = 0$ is a better assignment because we observe an even parity ground state, decay to which can only come from an odd parity PA state. The symmetry of the $J = 2$ rotational state is also odd, but we would expect $J = 2$ to lead to additional rotational structure in the present measurements.

While this interpretation of the depletion data presented here is consistent with other experimental data, it is not consistent with the available theory of the $d\ ^3\Pi$ state. The theory from Ref. 11 predicts $\Omega = 0^+$ should be lower in energy than $\Omega = 0^-$, while our interpretation of the data implies the opposite. One possible resolution to this problem is that we have incorrectly identified the ground state rotational level. If our ground state is $K'' = 1$ instead of $K'' = 0$, this would flip our $\Omega = 0^+$, 0^- ordering. However, this would require that p-wave is the dominant scattering partial wave, a scenario unsupported by Refs. 7 and 26 or the best available potential energy curves.[18] It is worth noting that in the $d\ ^3\Pi$ state in RbCs, a close analog, $\Omega = 0^-$ appears to be lower in energy than $\Omega = 0^+$.[12] Nevertheless, we find the poor agreement with theory unsettling.

We used these data to determine the spin-orbit splitting between the different Ω progressions deep in the $d\ ^3\Pi$ well and followed these progressions back to the asymptote in our RE2PI data. Most importantly, these data provide accurate locations of $v' = 0$ and 1, J' for future work on short range PA.[27]

The depletion data are limited by the shot noise in our ion counting. For each data point, we integrate 200 shots and usually count ~350 ions. To get 2σ resolution, the smallest depletion feature that we can be confident in has to be a 10% decrease. Here our on-resonance depletion signal drops by around 30% which is 6σ and statistically significant. Unfortunately, our Ti:sapphire struggles to tune to wavelengths much shorter than 740 nm, which limited our depletion spectra to the lowest two vibrational levels only. Despite these short comings, depletion spectroscopy gives us accurate identifications of these bottom two vibrational levels of the $d\ ^3\Pi$ electronic state and unambiguously determines the spin orbit splitting.

V. DISCUSSION

We determine the vibrational binding energies and rotational constants of the states seen in depletion spectroscopy, which we tabulate in Table I. We list in Table II the assignments and energy of each of the $d\ ^3\Pi$ states that we observe through RE2PI and depletion spectroscopy. We also include in this table the energy difference between adjacent states, which aids in the assignment of the lines.

The theoretical vibrational levels and spin-orbit splittings that we used to guide our work and for comparison of results

TABLE II. Experimental assignments for the rotationless energy of the vibrational levels of the $d\ ^3\Pi$ state based on our RE2PI data, aided by our depletion data for $v' = 0$ and 1. Uncertainty for all assignments is 0.5 cm^{-1}. We have referenced the term energies, T_v, to the Rb 5S + Li 2S asymptote.

	$d\ ^3\Pi_0$		$d\ ^3\Pi_1$		$d\ ^3\Pi_2$	
v'	T_v (cm^{-1})	ΔE (cm^{-1})	T_v (cm^{-1})	ΔE (cm^{-1})	T_v (cm^{-1})	ΔE (cm^{-1})
0	13 508.2	98.8	13 545.2	99.1	13 578.1	99.3
1	13 607.0	94.9	13 644.3	95.4	13 677.4	92.0
2	13 701.9	94.8	13 739.7	92.0	13 769.4	96.0
3	13 796.7	87.3	13 831.7	89.6	13 865.4	88.1
4	13 883.9	83.8	13 921.3	83.5	13 953.5	86.1
5	13 967.7	80.5	14 004.8	81.2	14 039.6	80.9
6	14 048.2	79.0	14 086.0	78.1	14 120.5	77.5
7	14 127.2	74.8	14 164.1	75.1	14 198.0	75.2
8	14 202.0	71.2	14 239.2	71.6	14 273.2	71.5
9	14 273.2	71.5	14 310.8	68.7	14 344.7	68.0
10	14 344.7	66.3	14 379.5	64.8	14 412.5	64.1
11	14 411.0	64.2	14 444.3	65.2	14 476.6	63.0
12	14 475.2	62.1	14 509.5	59.4	14 539.6	58.8
13	14 537.3	59.4	14 568.9	56.9	14 598.4	55.8
14	14 596.7	55.1	14 625.8	54.7	14 654.2	51.4
15	14 651.8	51.4	14 680.5	51.4	14 705.6	46.2
16	14 703.2	47.6	14 731.9	44.3	14 751.4	43.4
17	14 750.8	47.0	14 776.2	40.1	14 795.2	37.9
18	14 797.8	45.9	14 816.3	35.5	14 833.1	32.5
19	14 843.7	25.2	14 851.8	24.4	14 865.6	23.9
20	14 868.9	21.3	14 876.2	16.6	14 889.5	8.7
21	14 890.2	10.7	14 892.8	6.9	14 898.2	
22	14 900.9		14 899.7			

TABLE III. Molecular vibrational constants fitted to our data, $T(v) = T_e + \omega_e(v+1/2) - \omega_e x_e(v+1/2)^2 + \omega_e y_e(v+1/2)^3$, where $T(v)$ is the rotationless energy of the vth vibrational level. Additionally, $B_v = B_e - \alpha_e(v+1/2)$, where B_v is the rotational constant of the vth vibrational level. We set the α_e term to 0 because we had so few measurements of B_v and it is usually much smaller than B_v; the uncertainty has been increased to account for this. The uncertainty is given in parentheses. The theory values are from fitting the bound states calculated by LEVEL 8.0 using PECs from Ref. 11. When fitting the experimental data, we used only the $v' = 0$-19 to increase the accuracy.

	$d\,^3\Pi_0$		$d\,^3\Pi_1$		$d\,^3\Pi_2$	
	Expt.	Th.	Expt.	Th.	Expt.	Th.
T_e (cm^{-1})	13 459.2 (1.5)	13 300.7	13 497.5 (2.0)	13 359.9	13 528.0 (1.4)	13 398.2
ω_e (cm^{-1})	101.4 (0.7)	103.6	100.4 (0.9)	102.8	101.7 (0.6)	102.4
x_e (10^{-3})	16.7 (0.8)	13.1	15.0 (1.0)	12.7	15.8 (0.7)	12.5
y_e (10^{-3})	0.068 (0.028)	−0.06	−0.038 (0.033)	−0.10	−0.036 (0.026)	−0.12
B_e (cm^{-1})	0.148 (6)	0.159	0.153 (8)	0.159		0.159

come from *ab initio* calculations by Korek *et al.*[11] with aid from LEVEL 8.0.[21] We found good overall agreement with these *ab initio* results. The spin-orbit splittings for $\Omega = 0$ to $\Omega = 1$, predicted to be 21 cm^{-1}, are measured here to be 37 cm^{-1}; for $\Omega = 1$ to $\Omega = 2$, they are predicted to be 38 cm^{-1}, and we found them to be 33 cm^{-1}. For the spin-orbit splitting between the $\Omega = 0^+$ and $\Omega = 0^-$ states, however, we observe −0.9 cm^{-1}, significantly less than the predicted 36 cm^{-1} (and of the wrong sign). Our depletion data are unambiguous in establishing the magnitude of the $\Omega = 0^+$ to $\Omega = 0^-$ splitting, although it is possible we have the wrong sign, and a small $\Omega = 0^+$ to $\Omega = 0^-$ splitting is consistent with observations of similar states like the (3) $^3\Pi$ state in LiRb[8] and in KRb.[28]

We show the vibrational spacing, $\Delta E = E_{v+1} - E_v$ vs v, of the different series in Fig. 6. These data are in reasonable agreement with the predicted vibrational splittings although there appears to be a nearly uniform difference of a few cm^{-1}. We found that the depth of the $d\,^3\Pi$ potential (expt. value) is less than that predicted (th. value). We looked extensively for another vibrational level below our assigned $v' = 0$ level. We covered ±10 cm^{-1} around the expected vibrational location with our depletion spectra, but found no indication of a depletion resonance. The calculated FCF for the $d\,^3\Pi$ $v' = 0 \leftarrow a\,^3\Sigma^+$ $v'' = 13$ transition is comparable to the FCF for the $d\,^3\Pi$ $v' = 1 \leftarrow a\,^3\Sigma^+$ $v'' = 13$ transition, which implies that if another vibrational level exists, we would have found it.

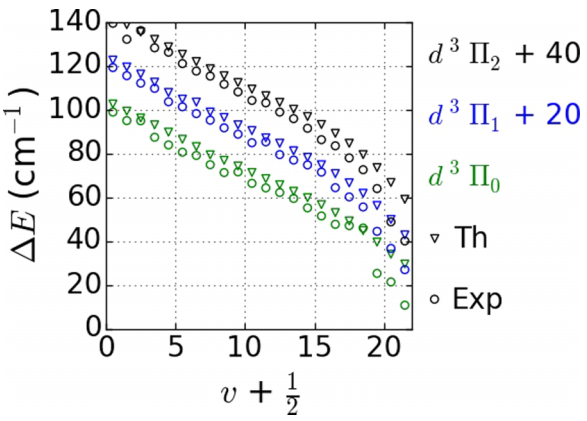

FIG. 6. Comparison of our extracted vibrational splitting to predicted vibrational splitting. The circles represent our data, while the triangles are predicted by *ab initio* curves.[11] Green markers label $\Omega = 0$ (compared to *ab initio* $\Omega = 0^+$) spacings. Blue markers are shifted by +20 cm^{-1} and label $\Omega = 1$ spacings. Black markers are shifted by +40 cm^{-1} and label $\Omega = 2$ spacings. We have shifted the $\Omega = 1$ and $\Omega = 2$ progressions (+20 cm^{-1} and +40 cm^{-1}) to make the different progressions more visible.

Our extracted molecular constants are listed in Table III. These provide an easy estimation of the spectral structure of the $d\,^3\Pi$ states as well as a quick comparison to theoretical predictions. As borne out in Fig. 6, there is good agreement between our fitted harmonic constant, ω_e, and the predictions. Additionally, there is good agreement between the rotational constants, B_e, extracted from the depletion spectra and the predictions. However, there is considerably less agreement between our extracted term energy, T_e, and the predictions for reasons discussed previously. Additionally, it is important to note that when we fitted the experimental data to determine T_e, ω_e, x_e, and y_e, we used only $v' = 0$-19. This increased the accuracy of the fit so that for these vibrational levels, our molecular constants reproduce our data with a standard deviation of 2 cm^{-1}. We believe that most of the deviations are caused by experimental uncertainties on determining the frequencies of the peaks, as well as small perturbations to state locations caused by spin-orbit mixing.

VI. CONCLUSION

In this work, we have found and identified the $v = 0$ to $v = 22$ states of the $d\,^3\Pi_\Omega$ electronic state in LiRb. We explored singlet-triplet mixing to evaluate the possibility of using the $d\,^3\Pi - D\,^1\Pi$ mixed states as the intermediate state in a STIRAP transfer from a weakly bound triplet state to deeply bound singlet states. We know from heat pipe spectra[18] and other REMPI data[9] that the transitions from deeply bound $D\,^1\Pi$ v' to deeply bound $X\,^1\Sigma^+$ states are strong. Our depletion data show that transitions from weakly bound triplet molecules to deeply bound $d\,^3\Pi_1$ v' states are also strong. Finally, our RE2PI data demonstrate that there is about 10% mixing between most of these singlet and triplet states. We suggest using the $d\,^3\Pi_1$ $v' = 0$ $J' = 1$ state as the intermediate state for a STIRAP transfer in future work. The laser wavelengths for this transfer would be 740 nm, achievable with Ti:sapphire or diode lasers, and 516 nm, which is accessible with green laser

diodes. Using calculated FCFs and an estimate of the transition dipole moment of a few times ea_0, the "up" transition would be around $4 \times 10^{-2}\ ea_0$ and the "down" transition would be around $10^{-2}\ ea_0$ which is competitive with the transfer strength used by the KRb JILA team.[29]

Using the binding energy of the lowest several vibrational levels, we have assessed their potential for short-range photoassociation. There are only six possible PA transitions we can observe with our current Ti:sapphire laser, the same six we saw in depletion. However, our depletion data provide the perfect stepping stone for this type of work, providing very trusted locations of vibrational levels (to within 0.5 cm^{-1}, the uncertainty in the binding energy of $a\ ^3\Sigma^+\ v'' = 13$). Of particular interest to us is the combination of short range PA and mixing between $d\ ^3\Pi$ and $D\ ^1\Pi$. This provides an avenue through simple spontaneous decay to the rovibronic ground state although we will need a different laser to access these PA resonances.

ACKNOWLEDGMENTS

We are happy to acknowledge useful conversations with Jesús Pérez-Ríos and university support of this work through the Purdue OVPR AMO incentive grant. And we would like to acknowledge the work done by S. Dutta and J. Lorenz in building the LiRb machine.

[1]G. Pupillo, A. Griessner, A. Micheli, M. Ortner, D.-W. Wang, and P. Zoller, Phys. Rev. Lett. **100**, 050402 (2008).
[2]D. DeMille, Phys. Rev. Lett. **88**, 067901 (2002).
[3]K.-K. Ni, S. Ospelkaus, D. Wang, G. Quéméner, B. Neyenhuis, M. De Miranda, J. Bohn, J. Ye, and D. Jin, Nature **464**, 1324 (2010).
[4]M. Aymar and O. Dulieu, J. Chem. Phys. **122**, 204302 (2005).
[5]S. Dutta, D. S. Elliott, and Y. P. Chen, Europhys. Lett. **104**, 63001 (2014).
[6]S. Dutta, J. Lorenz, A. Altaf, D. S. Elliott, and Y. P. Chen, Phys. Rev. A **89**, 020702 (2014).
[7]I. Stevenson, D. Blasing, Y. P. Chen, and D. S. Elliott, "Production of ultracold ground state LiRb molecules by photoassociation through a resonantly coupled state," Phys. Rev. A (to be published); e-print arXiv:1603.02567.
[8]A. Altaf, S. Dutta, J. Lorenz, J. Pérez-Ríos, Y. P. Chen, and D. S. Elliott, J. Chem. Phys. **142**, 114310 (2015).
[9]J. Lorenz, A. Altaf, S. Dutta, Y. P. Chen, and D. S. Elliott, Phys. Rev. A **90**, 062513 (2014).
[10]C. Marzok, B. Deh, C. Zimmermann, P. W. Courteille, E. Tiemann, Y. Vanne, and A. Saenz, Phys. Rev. A **79**, 012717 (2009).
[11]M. Korek, G. Younes, and S. Al-Shawa, J. Mol. Struct.: THEOCHEM **899**, 25 (2009).
[12]C. Gabbanini and O. Dulieu, Phys. Chem. Chem. Phys. **13**, 18905 (2011).
[13]T. Shimasaki, M. Bellos, C. Bruzewicz, Z. Lasner, and D. DeMille, Phys. Rev. A **91**, 021401 (2015).
[14]Z. Ji, H. Zhang, J. Wu, J. Yuan, Y. Yang, Y. Zhao, J. Ma, L. Wang, L. Xiao, and S. Jia, Phys. Rev. A **85**, 013401 (2012).
[15]S. Dutta, A. Altaf, J. Lorenz, D. S. Elliott, and Y. P. Chen, J. Phys. B: At., Mol. Opt. Phys. **47**, 105301 (2014).
[16]W. Ketterle, K. B. Davis, M. A. Joffe, A. Martin, and D. E. Pritchard, Phys. Rev. Lett. **70**, 2253 (1993).
[17]I. Stevenson, D. Blasing, Y. P. Chen, and D. S. Elliott, "The $C^1\Sigma^+$, $A^1\Sigma^+$, and $b^3\Pi_0^+$ states of LiRb," Phys. Rev. A (to be published); e-print arXiv:1609.08591.
[18]M. Ivanova, A. Stein, A. Pashov, H. Knöckel, and E. Tiemann, J. Chem. Phys. **134**, 024321 (2011).
[19]J. Lorenz, Ph.D. thesis, Purdue University, 2014.
[20]J. Ulmanis, J. Deiglmayr, M. Repp, R. Wester, and M. Weidemuller, Chem. Rev. **112**, 4890 (2012).
[21]R. J. Le Roy, "LEVEL: A computer program for solving the radial Schrödinger equation for bound and quasibound levels," J. Quant. Spectrosc. Radiat. Transfer **186**, 167 (2017).
[22]J. Deiglmayr, A. Grochola, M. Repp, K. Mörtlbauer, C. Glück, J. Lange, O. Dulieu, R. Wester, and M. Weidemüller, Phys. Rev. Lett. **101**, 133004 (2008).
[23]D. Wang, J.-T. Kim, C. Ashbaugh, E. E. Eyler, P. Gould, and W. C. Stwalley, Phys. Rev. A **75**, 032511 (2007).
[24]G. Herzberg, *Molecular Spectra and Molecular Structure, I. Spectra of Diatomic Molecules*, 2nd ed. (Krieger, Malabar FL, 1989).
[25]Because photoassociation followed by spontaneous decay to form molecules is a two photon process and selection rules dictate that parity needs to change for each transition, the ground state and the scattering state need to have the same parity.
[26]S. Dutta, private communication.
[27]D. Blasing, I. Stevenson, Y. P. Chen, and D. S. Elliott, "Short-range photoassociation of LiRb," Phys. Rev. A (to be published); e-print arXiv:1608.06648.
[28]J. Banerjee, D. Rahmlow, R. Carollo, M. Bellos, E. E. Eyler, P. L. Gould, and W. C. Stwalley, J. Chem. Phys. **138**, 164302 (2013).
[29]K.-K. Ni, S. Ospelkaus, M. De Miranda, A. Pe'er, B. Neyenhuis, J. Zirbel, S. Kotochigova, P. Julienne, D. Jin, and J. Ye, Science **322**, 231 (2008).